Counting actin in contractile rings reveals novel contributions of cofilin and type II myosins to fission yeast cytokinesis

Mamata Malla[a], Thomas D. Pollard[b,c,d], and Qian Chen[a,b,*]
[a]Department of Biological Sciences, The University of Toledo, Toledo, OH 43606; [b]Departments of Molecular Cellular and Developmental Biology, [c]Molecular Biophysics and Biochemistry, and [d]Cell Biology, Yale University, New Haven, CT 06520-8103

ABSTRACT **Cytokinesis by animals, fungi, and amoebas depends on actomyosin contractile rings, which are stabilized by continuous turnover of actin filaments. Remarkably little is known about the amount of polymerized actin in contractile rings, so we used low concentrations of GFP-Lifeact to count total polymerized actin molecules in the contractile rings of live fission yeast cells. Contractile rings of wild-type cells accumulated polymerized actin molecules at 4900/min to a peak number of ~198,000 followed by a loss of actin at 5400/min throughout ring constriction. In *adf1-M3* mutant cells with cofilin that severs actin filaments poorly, contractile rings accumulated polymerized actin at twice the normal rate and eventually had almost twofold more actin along with a proportional increase in type II myosins Myo2, Myp2, and formin Cdc12. Although 30% of *adf1-M3* mutant cells failed to constrict their rings fully, the rest lost actin from the rings at the wild-type rates. Mutations of type II myosins Myo2 and Myp2 reduced contractile ring actin filaments by half and slowed the rate of actin loss from the rings.**

Monitoring Editor
Karen Oegema
University of California, San Diego

Received: Aug 3, 2021
Revised: Sep 28, 2021
Accepted: Oct 1, 2021

INTRODUCTION

Cytokinesis separates daughter cells during the last stage of the cell cycle. Amoebas, fungi, and animal cells assemble an actomyosin ring to provide force to form a cleavage furrow (for review see Pollard and O'Shaughnessy, 2019). Contractile rings consist of actin filaments, actin-binding proteins including α-actinin, capping protein, cofilin, formins, and type II myosins (Wu *et al.*, 2003). In fission yeast, two type II myosins contribute about equally to the rate of ring constriction (Bezanilla *et al.*, 2000; Laplante *et al.*, 2015). Myo2 is essential for viability, while the unconventional myosin-II called Myp2 is not.

Although actin is the most abundant protein in contractile rings, much less is known about its dynamics than that of the myosins or actin-binding proteins owing to difficulty in tracking actin in live cells. Fluorescent phalloidin is widely used to stain actin in fixed cells, but this provides only a snapshot. SIR-actin, jasplakinolide conjugated to silicon rhodamine, can stain actin filaments in live cells (Lukinavicius *et al.*, 2014), but jasplakinolide will alter actin dynamics. Microinjection of fluorescently labeled actin is an option for some animal cells (Cao and Wang, 1990a) but has not been exploited for quantitative measurements and may not be feasible for some cells including fungi. Unfortunately, the genetically encoded fluorescent tags tested to date compromise the function of actin during cytokinesis. For example, the formins that nucleate and elongate actin filaments for the contractile ring in fission yeast filter out all the actin fused to either fluorescent proteins such as GFP or small tetracysteine peptide tags (Wu and Pollard, 2005; Chen *et al.*, 2012).

Consequently, only indirect labeling of actin filaments in the contractile ring has been successful. Although less versatile than direct labeling, we measured about 190,000 actin molecules, equal to 500 μm of actin filaments, in the fission yeast contractile ring by titration with Lifeact (Courtemanche *et al.*, 2016), a small peptide that binds actin filaments (Riedl *et al.*, 2008). We also estimated the average length of the filaments from the ratio of polymerized actin to formin

This article was published online ahead of print in MBoC in Press (http://www.molbiolcell.org/cgi/doi/10.1091/mbc.E21-08-0376) on October 6, 2021.

*Address correspondence to: Qian Chen (Qian.Chen3@UToledo.edu).

Abbreviations used: Adf1, actin depolymerizing factor 1; DMSO, dimethyl sulfoxide; EDTA, ethylenediaminetetraacetic acid ; EM, electron microscopy; LA, lifeact; PVDF, polyvinylidene fluoride; SD, standard deviation; SDS–PAGE, sodium dodecyl sulfate polyacrylamide gel electrophoresis; SIN, septation initiation network; WT, wild-type; YE5s, yeast extract with 5 supplements.

© 2022 Malla *et al.* This article is distributed by The American Society for Cell Biology under license from the author(s). Two months after publication it is available to the public under an Attribution–Noncommercial-Share Alike 4.0 International Creative Commons License (https://creativecommons.org/licenses/by-nc-sa/4.0).
"ASCB®," "The American Society for Cell Biology®," and "Molecular Biology of the Cell®" are registered trademarks of The American Society for Cell Biology.

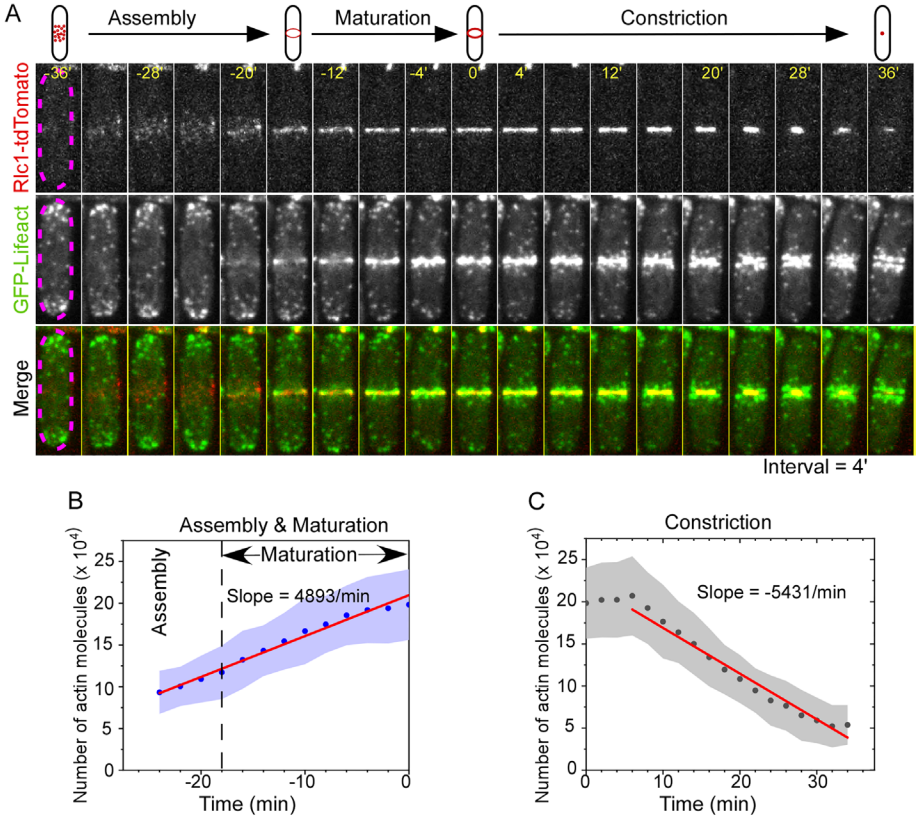

FIGURE 1: Counting the actin molecules in the contractile ring of fission yeast using GFP-Lifeact. (A) Assembly and constriction of the contractile ring documented by time-lapse micrographs of a wild-type cell expressing both GFP-Lifeact (top) and Rlc1-tdTomato (middle). A merged time-lapse series is shown at the bottom. Dashed lines represent the cell outline. (B, C) Average time course of the number of actin molecules in the contractile rings during (B) their assembly and maturation and (C) constriction in wild-type cells. Clouds represent SDs. Time zero is defined as the start of the ring constriction. Red line represents the best linear fit ($R^2 > 0.9$).

molecules in the contractile ring. The filaments start at about 1.4 µm and shorten gradually during the ring constriction. Despite this progress, little is known about how actin filaments themselves turn over in contractile rings.

Cofilins promote actin turnover during endocytosis in yeast (Okreglak and Drubin, 2007; Chen and Pollard, 2013), at the leading edge of motile cells (Konzok *et al.*, 1999; Ghosh *et al.*, 2004), and in neurite growth cones (Zhang *et al.*, 2012). This small actin-binding protein is required for the assembly of the cytokinetic contractile ring in fission yeast (Nakano and Mabuchi, 2006; Chen and Pollard, 2011). Cofilin mutations that reduce severing activity slow or prevent the assembly of contractile rings, because the precursors to the contractile ring, called cytokinetic nodes, are pulled into large heterogeneous clusters around the equator rather than being organized into a contractile ring. Rings that form slowly from these clusters constrict far more variably than those in wild-type cells (Chen and Pollard, 2011).

Here we expanded our previous study (Courtemanche *et al.*, 2016) to count polymerized actin in contractile rings of wild-type fission yeast and strains with mutations in cofilin, formin, and type II myosins. The cofilin mutant *adf1-M3* with half of wild-type severing activity had strong effects on both contractile ring assembly and disassembly. The contractile rings of the cofilin mutant cells have about twice the normal numbers of actin, formin Cdc12, Myo2, and Myp2 molecules, while contractile rings of cells with a hypomorphic mutation of formin Cdc12 accumulated actin slowly. Remarkably, mutations of either type II myosin, Myo2 or Myp2, reduced contractile ring actin by half.

RESULTS

Measurement of actin turnover in contractile rings using GFP-Lifeact

To measure the number of polymerized actin molecules in contractile rings of live fission yeast over time, we expressed GFP-Lifeact (GFP-LA) constitutively from the endogenous *leu1* locus, driven by a constitutive *Padf1* promoter of the endogenous cofilin gene. All yeast strains used in this study expressed GFP-LA at similar levels (Supplemental Figure S1), which saturates only 6% of polymerized actin molecules and avoids artifacts during cytokinesis and endocytosis caused by higher concentrations of GFP-Lifeact (Courtemanche *et al.*, 2016). Using a calibrated fluorescence microscope (Wu and Pollard, 2005), we converted the fluorescence intensity of GFP-Lifeact into the numbers of actin molecules in subcellular structures (Courtemanche *et al.*, 2016). Additionally, we expressed from the endogenous locus Rlc1, the regulatory light chain for both Myo2 and Myp2, tagged with tdTomato (Rlc1-tdTomato) and used its fluorescence to segment the contractile ring and measure the total GFP-Lifeact fluorescence.

Actin accumulated in contractile rings, about half during assembly and about half during 18 min of maturation when the rate was constant at ~4900 molecules/min (Figure 1, A and B, and Table 1). At the end of the maturation phase, just before cleavage furrow ingression, fully assembled contractile rings contained ~198,000 polymerized actin molecules, consistent with previous measurements (Courtemanche *et al.*, 2016).

During contractile ring constriction the number of polymerized actin molecules was constant for the first 6 min, which was not clear in our previous analysis (Courtemanche *et al.*, 2016), and then declined steadily at ~5400 molecules/min for ~20 min (Figure 1C). About 50,000 actin molecules remained in the contractile ring remnant at the end of constriction, which has not been reported previously. These filaments abruptly dispersed within 2 min, together with Rlc1-tdTomato, leaving behind actin patches along both sides of the cleavage furrow (Figure 1A).

Contractile ring assembly and composition in the cofilin hypomorphic mutant *adf1-M3*

Cofilin is essential for viability, so we used the hypomorphic mutant *adf1-M3* to test the role of cofilin in the dynamics of contractile ring actin filaments. The *adf1-M3* mutation reduces the severing activity of cofilin by more than 50% and slows contractile ring assembly (Chen and Pollard, 2011). Actin patches and actin filament bundles stained brighter with Bodipy-phallacidin in fixed *adf1-M3* mutant cells than in wild-type cells (Chen and Pollard, 2011). However, at that time we lacked quantitative probes to measure polymerized

Genotype	Number of actin molecules in the mature ring (×10³)[a]	Number of cells measured[a]	Net assembly rate (actin molecules × 10³ min⁻¹)[b]	Net disassembly rate (actin molecules × 10³ min⁻¹)[b]	Normalized disassembly rate (percent min⁻¹)[c]
Wild type	198 ± 42	80	+4.9	–5.4	–2.7
adf1-M3	362 ± 176	21	+10.0	–5.8	–1.6
cdc12-4A	93 ± 23	38	+2.4	N.M.[d]	N.M.
myo2-E1	82 ± 28	38	N.M.	–1.6	–2.0
myp2Δ	88 ± 21	33	N.M.	–2.3	–2.6

[a]The cells were pooled from at least two independent biological repeats.
[b]Based on the best fits of linear regression. $R^2 > 0.90$.
[c]Equals the net disassembly rate divided by the total number of actin molecules in the ring.
[d]N.M.: Not measured.

TABLE 1: Summary of the actin assembly and disassembly in the contractile ring.

actin in live cells (Chen *et al.*, 2012). The cytokinesis defects were less severe in the *adf1-M3* strain than in *adf1-M2* (Chen and Pollard, 2011), allowing us to analyze the assembly and disassembly of larger numbers of mature rings.

Contractile ring assembly in *adf1-M3* mutant cells was less orderly (Figure 2B) and much more variable than in wild-type cells (Figure 2, B–D). Contractile rings of *adf1-M3* mutant cells accumulated actin twice as fast over a similar period of time as wild-type cells (Table 2). Therefore, mature rings of the mutant had on average about 1.9 times as much actin as wild-type cells (Table 1 and Figure 2A, arrows). The peak number of molecules (100,000–600,000) was much more variable in *adf1-M3* mutant cells than in wild-type cells (Figure 2D). On average, the contractile rings of *adf1-M3* mutant cells had enough actin molecules to assemble ~950 µm of filaments (Table 2). A cross-section of such rings would contain ~75 filaments in a bundle ~160 nm wide, if the spacing between the actin filaments is 15 nm as in wild-type cells, which have ~50 filaments in a bundle ~125 nm wide (Courtemanche *et al.*, 2016; Swulius *et al.*, 2018). We conclude that severing by cofilin limits and ensures reliable assembly of actin filaments in the contractile ring.

To estimate the lengths of actin filaments in the contractile ring of *adf1-M3* mutant cells, we measured the number of formins in fully assembled contractile rings just before they constricted. Assuming that barbed ends of all contractile ring actin filaments are associated with a formin (Coffman *et al.*, 2013), the ratio of total actin to total formin molecules gives the average length of actin filaments, averaging ~1.5 µm in wild-type cells (Table 2), similar to the previous estimate (Courtemanche *et al.*, 2016).

The number of Cdc12-3GFP molecules in the contractile rings of *adf1-M3* mutant cells was on average about twice that of wild-type cells and much more variable (Figure 3C), while the number of formin For3 was the same as in wild-type cells (Figure 3D). As a result, the combined number of the two formin molecules was ~50% higher in the contractile rings of the mutant cells (Table 2). Consequently, the ratio of actin to formins was ~25% higher, translating to an average length of 1.9 µm in the mutant cells (Table 2).

The numbers of type II myosins (Myo2 and Myp2) in mature contractile rings of wild-type cells peaked at ~7000 myosin molecules (Figure 3, A and B, and Table 2), consistent with previous measurements (Wu and Pollard, 2005; Goss *et al.*, 2014). This translates to one myosin motor domain for every 76 nm of actin filament and ~20 motor domains for every actin filament in the contractile ring.

Contractile rings of *adf1-M3* mutant cells that were able to constrict had twice as many myosin molecules as the wild-type cells, translating to one myosin motor domain for every 70 nm of filament (Figure 3, A and B, and Table 2). We conclude that reduced severing by cofilin leads to contractile rings with twice the normal numbers of actin, Cdc12, and type II myosin molecules, so the ratios of these three proteins are about the same as in wild-type cells.

Effects of a formin mutation on contractile ring assembly

Measurements of the time course of actin accumulation in the contractile rings of the *cdc12-4A* formin mutant cells identified defects in actin that were not appreciated in previous work (Bohnert *et al.*, 2013). The essential formin Cdc12 is required for assembly of actin filaments in contractile rings (Chang *et al.*, 1996; Kovar *et al.*, 2003). The hypomorphic *cdc12-4A* mutation prevents the phosphorylation of the formin by the essential SIN pathway kinase Sid2 (Bohnert *et al.*, 2013). In prior work the mutant cells appeared to assemble normal contractile rings, but our quantitative measurements revealed that the *cdc12-4A* mutation reduced by about half both the rate of accumulation and the peak numbers of polymerized actin in the ring (Figure 2E and Table 1).

Contractile ring disassembly during constriction in *adf1-M3* mutant cells

The contractile rings in 30% of *adf1-M3* mutant cells ($n = 65$) either failed to constrict or halted constriction prematurely (Supplemental Figure S2), but those that constricted fully did so at an average rate similar to that of wild-type cells although with much more variability (Chen and Pollard, 2011). During ring constriction, the absolute number of actin molecules in the contractile rings of *adf1-M3* cells declined linearly at ~5800/min (Figure 4, A and B, and Table 1), almost identical to the rate in wild-type cells. However, the cofilin mutant cells had two defects. First, the large standard deviations showed that rate of actin disassembly varied much more in *adf1-M3* cells than in wild-type cells. Second, the normalized disassembly rate, which took the number of actin molecules in the ring into consideration, was 40% lower in the mutant than in wild-type cells. Thus, normal severing by cofilin is not essential for the disassembly of actin filaments in constricting contractile rings but makes the process much more orderly.

Wild-type cells retain both Myo2 (Figure 4C) and Myp2 (Figure 4D) in the contractile ring through the first 20 min of constriction before they leave during the last 10 min of the constriction as observed earlier (Wu and Pollard, 2005). In contrast, these myosins persisted at nearly their highest levels for 1 h, and the time course of the process was much more variable in the *adf1-M3* mutant cells (Figure 4, C and D). In a few cofilin mutant cells, the myosins dwelled at the cell division site for more than 10 min after the completion of the ring constriction (Figure 5A). Myp2 oscillated as clusters along the contractile ring of the mutant cells, which was rarely observed in the wild-type cells (Figure 5A).

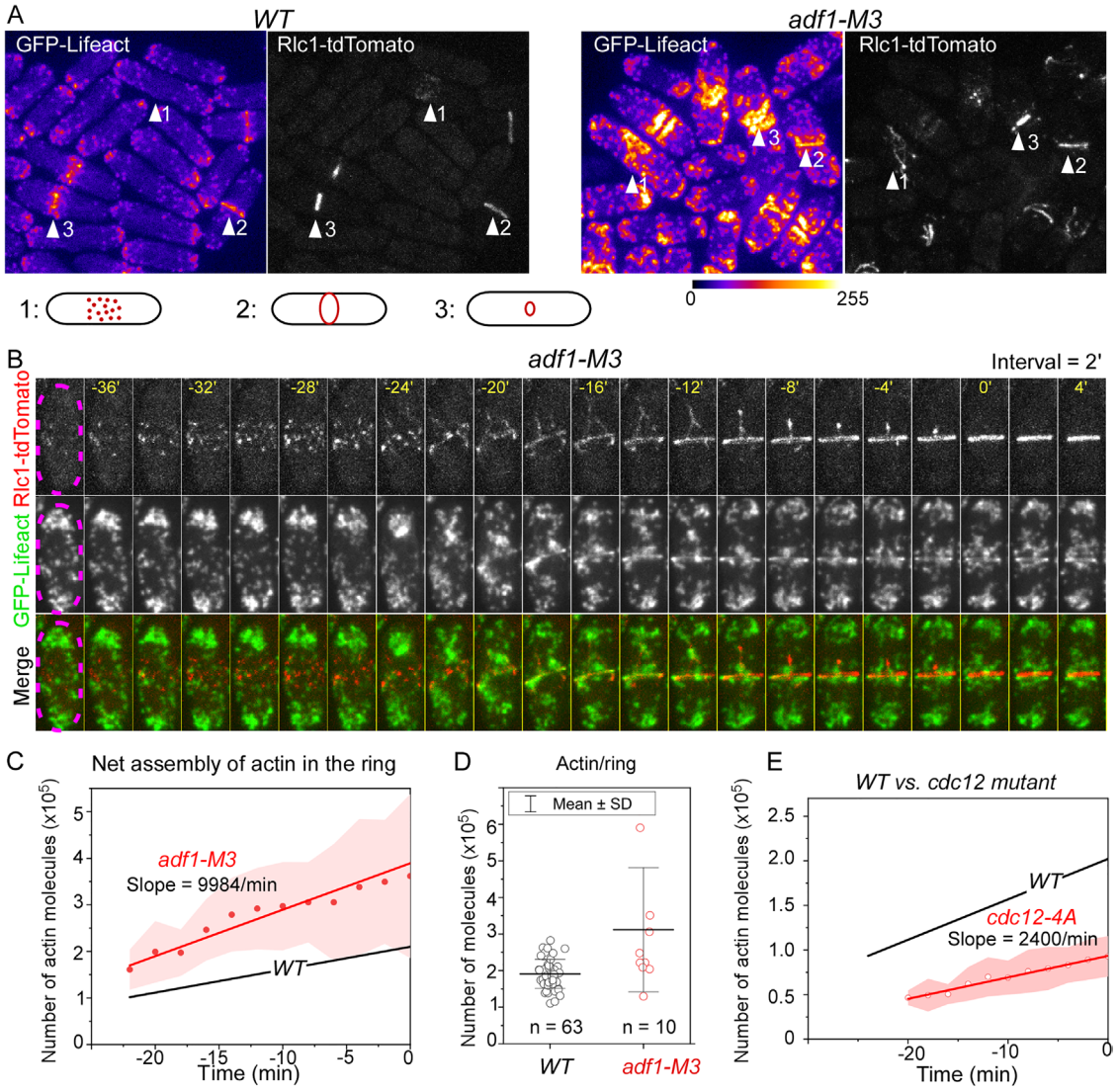

FIGURE 2: Contractile ring assembly in cofilin mutant *adf1-M3* and formin mutant *cdc12-4A*. (A) Fluorescence micrographs of the wild-type (left) and *adf1-M3* (right) cells. Both expressed GFP-Lifeact (pseudo colored) and Rlc1-tdTomato. Arrowheads: contractile rings at the stage of 1) assembly, 2) maturation, and 3) constriction. Bar represents the fluorescence intensity scale. (B) Time series of micrographs of a cofilin mutant cell expressing both GFP-Lifeact (top) and Rlc1-tdTomato (middle). A merged time-lapse series is shown at the bottom. (C) Average time course of actin molecules accumulating in the contractile rings of *adf1-M3* cells ($n = 21$). Red symbols are mean values; the line represents best linear fit ($R^2 > 0.9$); the cloud represents SDs. The line for WT is from Figure 1B. (D) Average number of actin molecules in mature contractile rings. Measurements were taken just before the start of the ring constriction. (E) Average time course of actin assembly in the contractile rings of *cdc12-4A* cells. The line is the best linear fit ($R^2 > 0.9$). The line for WT cells is from Figure 1B. The slope of *cdc12-4A* is significantly smaller than that of the wild type ($P < 0.005$).

Genotype	Estimated assembly time of actin (min)[a]	Total filament length in the mature ring (μm)	Number of formin dimers in the mature ring[b]	Number of type II myosin motor domains in the mature ring[c]	Average filament length in the mature ring (μm)[d]
Wild-type	43	530	~350	~7000	1.5
adf1-M3	39	975	~520	~14,000	1.9

[a]Based on the best fit of linear regression. Time = Number of actin molecules/net assembly rate.
[b]Based on the peak numbers of formins in the contractile ring (Figure 3, C and D).
[c]Based on the peak numbers of type II myosins in the contractile ring (Figure 3, A and B).
[d]Derived from division of the total filament length by the number of formin, For3 plus Cdc12, dimers.

TABLE 2: Comparison of the architecture of the contractile ring between wild type and the cofilin mutant.

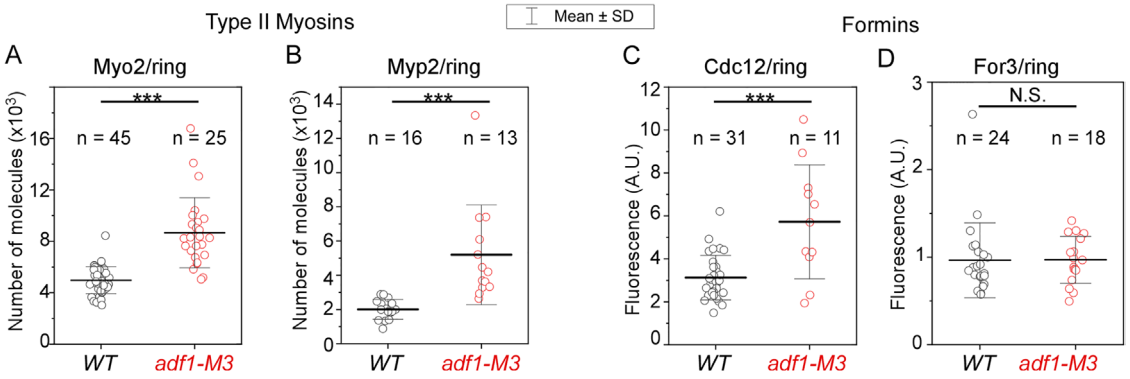

FIGURE 3: Architecture of the mature contractile ring in cofilin mutant cells. Related to Table 2. All measurements were taken just before the start of the ring constriction. (A, B) Numbers of type II myosins (A) Myo2 and (B) Myp2 in contractile rings of wild-type and *adf1-M3* cells. (C, D) The fluorescence intensities of two formins (C) Cdc12-3GFP and (D) For3-3GFP in contractile rings of wild-type and *adf1-M3* cells. ***, $P < 0.001$, N.S., $P > 0.05$. Values were calculated from two-tailed Student's *t* tests.

Face views of constricting contractile rings of *adf1-M3* cells revealed linear structures containing both myosin-II isoforms and actin filaments that separated from 60% ($n = 18$) of the rings (Figure 5, B and C). Similar structures were observed previously in three-dimensional reconstructions of cofilin mutants *adf1-M2* and *-M3* (Chen and Pollard, 2011; Cheffings *et al.*, 2019). Although the structures containing myosin-II retracted back to the contractile ring, the bundles of actin filaments did not (Figure 5C, arrowheads). Such shedding of actin filaments was not observed in the wild-type cells. We conclude that contractile rings are far less stable in cofilin mutant cells than in wild-type cells.

Influence of type II myosins on assembly and disassembly of contractile ring actin filaments

Mutations of either type II myosin gene in the *myo2-E1* or *myp2Δ* strains reduced the numbers of actin molecules in contractile rings by more than half compared with wild-type cells at the end of the maturation period and the onset of constriction (Figure 6, A and B, and Table 1). This surprising finding was missed previously.

Starting with less than the normal amount of polymerized actin, contractile rings constricted slower in both *myo2-E1* (0.32 μm/min) and *myp2Δ* (0.30 μm/min) cells than in wild-type cells (0.36 μm/min).

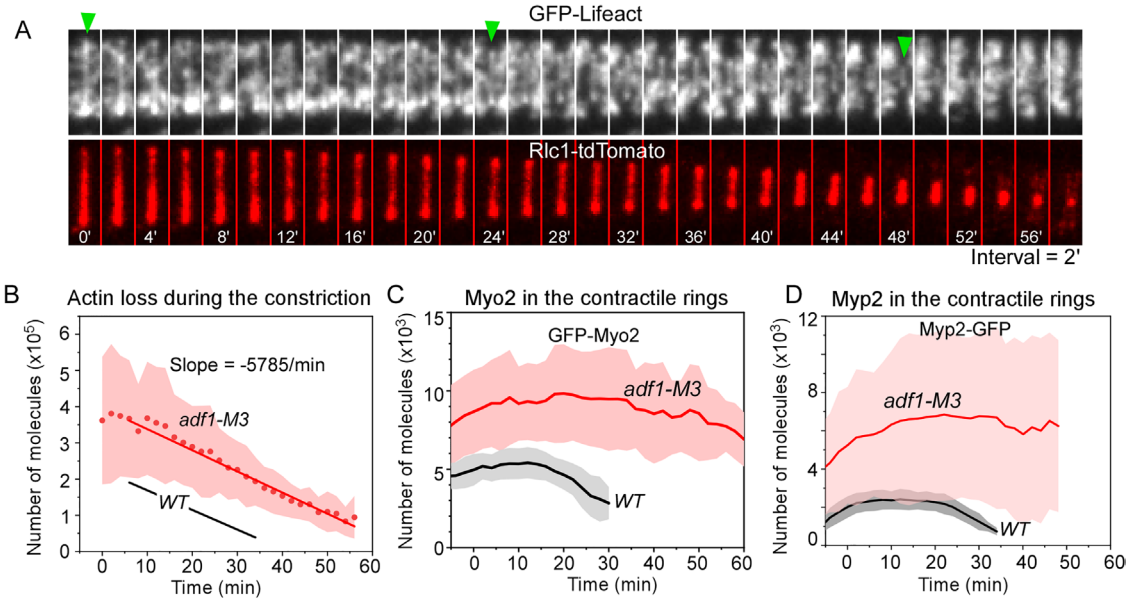

FIGURE 4: Time courses of the numbers of actin and type II myosins in constricting contractile rings of WT and *adf1-M3* cells. Time zero is the onset of constriction. (A) Time series of micrographs of a constricting contractile ring (arrowhead) in an *adf1-M3* mutant cell expressing GFP-Lifeact (top) and Rlc1-tdTomato (bottom, red). Interval = 2 min. (B) Average time course of the loss of actin molecules from contractile rings as they constricted. Red symbols are mean values; the line represents the best linear fit ($R^2 > 0.9$); the cloud shows SDs. The line for WT cells is from Figure 1C. (C, D) Average time course of the numbers of GFP-Myo2 (C) (WT [$n = 48$], *adf1-M3* [$n = 26$]) or Myp2-GFP (D) (WT [$n = 16$], *adf1-M3* [$n = 9$]) molecules in constricting contractile rings of WT and *adf1-M3* cells. The thick lines are mean values; the cloud shows SDs.

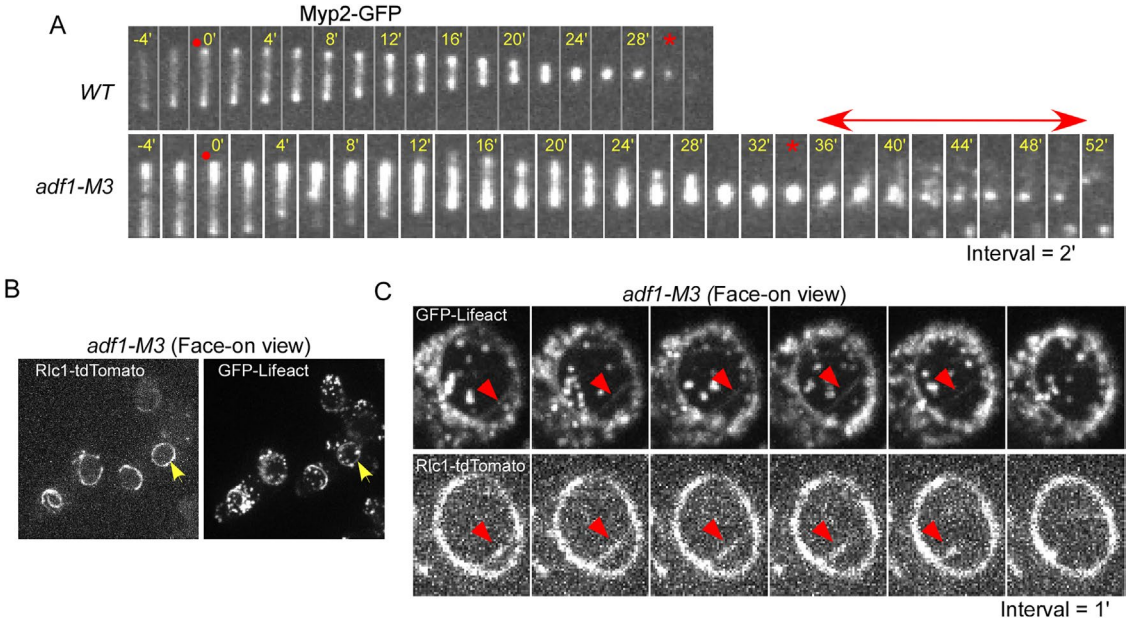

FIGURE 5: Disassembly of myosins in the contractile ring of the cofilin mutant. (A) Time series of micrographs of contractile rings in wild-type and *adf1-M3* cells expressing Myp2-GFP. Dot: onset of ring constriction. Asterisk: completion of ring constriction. Double-headed arrow: dwell time of the myosin remnant after the ring constriction. (B) Micrographs of *adf1-M3* cells expressing GFP-Lifeact (left) and Rlc1-tdTomato (right) in a Petri dish. (C) Time series of micrographs of the contractile ring in a cofilin mutant cell expressing GFP-Lifeact (top) and Rlc1-tdTomato (bottom). Arrowhead: shedding actin filaments (top panel) and myosin (bottom panel) from the contractile ring. The spots around the contractile ring are actin patches.

These rates are slightly higher than in earlier studies (Laplante *et al.*, 2015; Zambon *et al.*, 2017). After normalization for the initial actin content, the rates that actin left constricting rings were only slightly less than normal in the *myo2-E1* mutant and similar in the *myp2Δ* strain to that in wild-type cells (Table 1).

To rule out the possibility that the lower disassembly rates in the myosin mutants were indirectly tied to ring assembly defects, we measured the loss of actin from contractile rings of wild-type cells treated with blebbistatin to inhibit myosin-II (Straight *et al.*, 2003). Contractile rings in wild-type cells either disintegrated or failed to assemble in blebbistatin concentrations of ≥20 μM (Figure 6D). Treating wild-type cells with mature contractile rings with 10 μM blebbistatin decreased the rate of actin disassembly by 60% (Figure 6C). The ring constriction rate was also lower by 30% (n = 16) (Figure 6D). We conclude that type II myosins contribute to both the assembly and disassembly of actin filaments in contractile rings.

DISCUSSION

Knowing the numbers and dynamics of polymerized actin molecules in the actomyosin contractile ring is essential for understanding the mechanism of cytokinesis, but such measurements have not been made due to the technical challenge of labeling actin directly without disrupting its activity (Wu and Pollard, 2005; Chen *et al.*, 2012). Overexpression of indirect probes can produce artifacts, so we measured polymerized actin with a low concentration of GFP-Lifeact that does not perturb endocytosis or cytokinesis (Courtemanche *et al.*, 2016). Measurements on beautiful electron microscopy-tomograms (Swulius *et al.*, 2018) confirmed our earlier count of contractile ring actin with GFP-Lifeact (Courtemanche *et al.*, 2016).

Our method provides valuable, new quantitative data on the accumulation and loss of polymerized actin in contractile rings but does not reveal the behavior, including the turnover, of individual filaments. Experiments with a probe directly on actin molecules are required to probe the underlying mechanisms.

Our measurements revealed several aspects of cytokinesis that were overlooked due to the lack of quantitative data on actin in contractile rings, including the phenotypes of yeast strains with mutations in cofilin, myosin, and formin genes. The protein products of each of these genes are essential for cytokinesis, and their roles are likely to have been conserved during evolution.

The role of cofilin in the assembly and composition of contractile rings

A mutation that reduces the severing activity of cofilin has a remarkable impact on the molecular composition of the contractile ring: about twice the wild-type numbers of polymerized actin, Myo2, Myp2, and formin Cdc12. First, we consider myosins and then formins and actin for discussion.

Myosins. Myo2 and formin Cdc12 are components of cytokinesis nodes that form before the assembly of actin filaments (Wu and Pollard, 2005), so extra numbers of myosins in the contractile rings of *adf1-M3* cells implies proportionally more cytokinesis nodes. In fact, the nodes are larger in *adf1-M3* mutant cells than in wild-type cells (Chen and Pollard, 2011) and likely represent clusters of larger numbers of small, unitary nodes as revealed in wild-type cells by super-resolution microscopy (Laplante *et al.*, 2016). We do not know when these extra nodes form or how either reduced severing or more polymerized actin induce their formation.

On the other hand, Myp2 is recruited to fully formed contractile rings during the maturation period in a process that depends on actin filaments (Wu *et al.*, 2003; Takaine *et al.*, 2015; Okada *et al.*, 2019). Thus, the higher numbers of Myp2 molecules in the contractile ring of *adf1-M3* cells may follow directly from the high content of actin filaments.

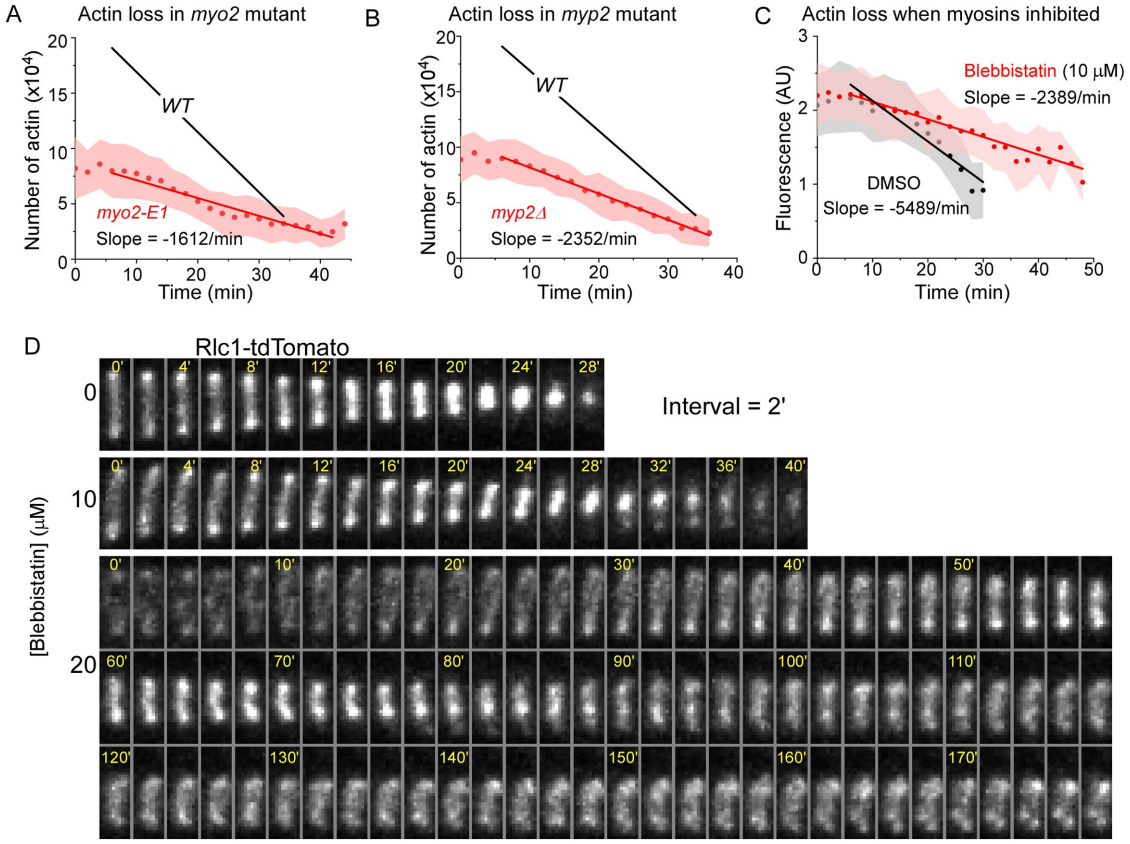

FIGURE 6: Disassembly of contractile ring actin filaments in type II myosin mutants at the permissive temperature of 22°C. (A, B) Average time courses of actin loss from constricting contractile rings of (A) *myo2-E1* and (B) *myp2Δ* mutant cells. Dark red circles are mean values; red lines are the best linear fits ($R^2 > 0.9$); the cloud shows SDs. The line for WT cells is from Figure 1C. (C) Time courses of GFP-Lifeact fluorescence in contractile rings of the cells treated with either 10 μM blebbistatin ($n = 16$) or 1% DMSO (control, $n = 25$). Only cells with a mature contractile ring before the treatment were included. Circles are mean values; solid lines are the best linear fits ($R^2 > 0.9$); the cloud shows SDs. (D) Time series of micrographs of contractile rings marked by Rlc1-tdTomato in three wild-type cells treated with either DMSO (top) or 10 μM (middle) or 20 μM (bottom) blebbistatin. Time zero represents the start of ring constriction except for 20 μM blebbistatin-treated cell in which time zero represents the start of the treatment.

Formins and actin. The essential formin Cdc12 nucleates and elongates actin filaments in the contractile ring (Chang *et al.*, 1996; Kovar *et al.*, 2003), so more formin Cdc12 in contractile rings of *adf1-M3* cells likely contributes to the rapid accumulation of extra actin filaments, and the actin monomer concentration in the cytoplasm sets the rate of growth of individual filaments. On the other hand, no connection between slow severing and excess formin is known.

The longer actin filaments in the contractile rings of *adf1-M3* cells are expected for cells with low actin filament severing activity (Chen and Pollard, 2011) and given evidence that cofilin stochastically severs actin filaments connecting the precursor nodes (Chen and Pollard, 2011). Longer filaments may also explain our observation of a negative genetic interaction between cofilin and α-actinin (*ain1*) mutants (Chen and Pollard, 2011).

Because actin filaments accumulate faster in the contractile rings of *adf1-M3* mutant cells, some other mechanism must account for the slow assembly of full contractile rings (Chen and Pollard, 2011). The most likely mechanism is that slow severing results in the aggregation of nodes that delays the coalescence of the nodes into an organized contractile ring of actin oligomers (Chen and Pollard, 2011).

In contrast to the essential formin Cdc12, *adf1-M3* cells do not accumulate excess formin For3, which is not a component of cytokinesis nodes and joins fully assembled contractile rings at a later stage and assembles peripheral actin bundles at the cell division plane (Coffman *et al.*, 2013). Unlike Cdc12, its recruitment likely depends on the type V myosins and polarized membrane secretion (Coffman *et al.*, 2013).

The role of cofilin in contractile ring constriction and disassembly

Multiple defects appear during constriction of contractile rings of *adf1-M3* cells. First, constriction is much less uniform than in wild-type cells. About 30% of the rings fail to complete the constriction. Bundles of actin filaments containing myosins peel from the rings of mutant cells. Second, starting with contractile rings containing much more polymerized actin and both type II myosins, the cofilin mutant cells required more time for all three proteins to leave the rings in a highly variable manner. Third, type II myosin Myp2 oscillates along the contractile rings as clusters. Nevertheless, the *adf1-M3* mutation does not significantly reduce the rate of net loss of actin filaments from contractile rings as they constrict.

The most likely explanation for the variability of contractile ring constriction in the *adf1-M3* cells is that the loss of severing activity

compromises the continuous, relatively rapid (tens of seconds) turnover of contractile ring components, which is required to maintain orderly force production in computer simulations of constriction (Stachowiak *et al.*, 2014). Those simulations assume estimates of continuous protein turnover revealed by photobleaching experiments. Dialing down the turnover of polymerized actin, Cdc12 and Myo2 in these simulations, resulted in the loss of tension in less than 3 min. Cofilin contributes to this turnover by severing actin filaments, while other uncharacterized processes cause the exchange of Cdc12 and Myo2 with cytoplasmic pools.

Role of formins in the assembly of the contractile ring

Counting polymerized actin revealed unrecognized defects caused by the *cdc12-4A* mutation. This mutation prevents phosphorylation of Cdc12 by the SIN pathway kinase Sid2 but does not cause any discernible cytokinetic defects (Bohnert *et al.*, 2013). Although cytokinesis appears normal, contractile rings in *cdc12-4A* mutant cells accumulate actin slower and in less than half the number of wild-type cells. This previously overlooked actin assembly defect may explain the hypersensitivity of this strain to latrunculin A as well as the genetic interaction of the *cdc12-4A* mutation with many other cytokinetic mutants (Bohnert *et al.*, 2013).

Roles of type II myosins in the assembly of the contractile ring

Our experiments revealed to our surprise that mutations of type II myosins strongly reduce the actin content of contractile rings. This remarkable, unexpected finding had been missed in dozens of studies on these mutant strains due to the lack of methods to measure actin in live cells. During ring assembly, Myo2 in a given node pulls on actin filaments growing from nearby nodes (Vavylonis *et al.*, 2008). In a reconstituted system, force on a filament growing from formin Cdc12 slows its elongation (Zimmermann *et al.*, 2017). However, the loss of Myo2 activity in the *myo2-E1* mutant has the opposite effect, resulting in more actin filaments, so the mechanism reducing the actin content is not clear. Myp2 is not present in contractile rings until after they form, so it must have its effect on the half of the actin that assembles during the maturation period, which is slower in the *myp2Δ* mutant than in wild-type cells.

In animal cells, the cortical flow of actin filaments toward the cleavage furrow contributes preformed actin filaments to the contractile ring (White and Borisy, 1983; Cao and Wang, 1990b; Khaliullin *et al.*, 2018). Nonmuscle type II myosins drive this flow by compressing the equatorial cortex (Khaliullin *et al.*, 2018). In comparison, fission yeast do not have an actin filament cortex, so formin Cdc12 associated with cytokinesis nodes assembles most of the contractile ring actin filaments de novo. Additional actin filaments in bundles formed by formin Cdc12 are also pulled into the ring from nonequatorial regions of dividing cells by Myo2 and Myo51 (Huang *et al.*, 2012). Therefore, our finding that the accumulation of actin filaments in the contractile ring depends on myosins exhibits some parallels with the cortical flow process in animal cells.

The role of type II myosins in constriction and disassembly of the contractile ring

Contractile rings with half the normal number of actin filaments constrict 10% slower in the *myo2-E1* strain and 20% slower in the *myp2Δ* strain than in wild-type cells (Laplante *et al.*, 2015). Disassembly of actin filaments is slower in both myosin mutants than in wild-type cells, although these rates are the same as in wild type when normalized for the starting actin content. Previously, the defects in ring constriction in the strains with myosin-II mutations were attributed entirely to loss of function of the myosins (Laplante *et al.*, 2015; Zambon *et al.*, 2017). However, these strains have a secondary defect, a loss of about half the normal polymerized actin. This insight emphasizes the importance of quantitative measurements of other contractile ring components in mutant strains.

Inhibition of myosins with 10 μM blebbistatin reduced both the disassembly rate of actin filaments and the ring constriction rate by ~60% and 30%, respectively. In addition to cofilin-mediated severing, forces produced by myosins may contribute to actin filament turnover during contractile ring constriction. The idea that such mechanical stress contributes to depolymerization/severing of actin filaments in contractile rings originated in experiments on sea urchin and *Caenorhabditis elegans* embryos (Schroeder, 1972; White and Borisy, 1983) and was supported by later work on animal cells in culture, where blebbistatin caused contractile ring actin filaments to turn over more slowly and persist longer than normal (Guha *et al.*, 2005; Murthy and Wadsworth, 2005). Further studies of cofilin mutants are essential to determine whether severing of actin filaments contributes to the disassembly of the contractile ring in animal cell cytokinesis.

Collectively, our experiments demonstrate the value of measurements of polymerized actin in live cells. These measurements provided new, unanticipated features of contractile ring assembly and constriction, which will motivate future studies to characterize mechanisms.

MATERIALS AND METHODS

Request a protocol through *Bio-protocol*.

Yeast genetics

We followed the standard protocols for yeast cell culture and genetics. Tetrads were dissected using a SporePlay+ dissection microscope (Singer, UK). Supplemental Table S1 lists all the strains used in this study.

Microscopy

For microscopy, exponentially growing yeast cells (1 ml) at 25°C with a density between 5.0×10^6/ml and 1.0×10^7/ml in YE5s (yeast extract with 5 supplements) liquid media were harvested by centrifugation at 4000 rpm for 1 min and resuspended in 50 μl YE5s. Owing to slow growth of the *adf1-M3* cells at 25°C, they were inoculated at 30°C for 1 d before being transferred to 25°C for inoculation of at least 12 h. Resuspended cells (6 μl) were applied to a 25% gelatin pad in YE5s and sealed under coverslip with VALAP (a mix of an equal amounts of Vaseline, lanolin, and paraffin) (Wang *et al.*, 2016).

Live cell microscopy was carried out on a calibrated Olympus IX71 microscope equipped with two objective lenses (Olympus; Plan Apochromat, 100 × [NA = 1.41] and 60 × [NA = 1.40]), a confocal spinning-disk unit (CSU-X1; Yokogawa, Japan), and a motorized XY stage with a Piezo Z Top plate (ASI). The images were captured on an Ixon-897 EMCCD camera controlled by iQ3.0 (Andor, Ireland). Solid-state lasers of 488 and 561 nm were used. In all experiments, the cells were imaged for 3 h with 2-min intervals. A Z-series of 15 slices at a step size of 0.5 μm was captured at each time point. The exceptions were measurement of the fluorescence of Cdc12-3GFP and For3-3GFP, for which Z-series of eight slices with a spacing of 1 μm were captured. Live cell microscopy was conducted in a room where the temperature was maintained at 22 ± 2°C. To minimize the experimental variations between the control and experimental groups, we imaged them with randomized order within 1 wk.

To obtain a face-on view of the contractile ring, yeast cells were imaged in a Petri dish with a coverslip at the bottom. Exponentially

growing cell culture (20 µl) was spotted onto the glass coverslip (#1.5) in a 10-mm Petri dish (Cellvis, USA). The coverslip was precoated with 50 µl of 50 µg/ml lectin (Sigma; L2380) and dried overnight at 4°C. The cells were allowed to attach to the coverslip for 10 min at room temperature before 2 ml of YE5s medium was added.

To treat the cells with blebbistatin, 20 µl of the cell culture was spotted onto a glass coverslip bottomed Petri dish as described above. We then added 2 ml of YE5s medium with either blebbistatin (from a 2 mM stock solution in dimethyl sulfoxide [DMSO]) or DMSO to the dish. The time series was started exactly 15 min afterward.

Image processing and analysis

We used ImageJ (National Institutes of Health) to quantify all the images, with either freely available or customized macros/plug-ins. The fluorescence micrographs were first corrected for *X–Y* drifting using the StackReg plug-in (Thevenaz *et al.*, 1998). We employed a customized Macro Tool to measure the fluorescence of GFP-Lifeact in the constricting rings (Courtemanche *et al.*, 2016). Maximum-intensity projections of the fluorescence of Rlc1-tdTomato were used for segmenting the contractile ring. To determine the start of ring closure, we constructed fluorescence kymographs of the constricting rings. Average intensity projections of the fluorescence of GFP-Lifeact were used to measure the number of actin molecules. After the background fluorescence was subtracted, the fluorescence intensities of GFP-Lifeact were converted to the number of actin molecules based on the calibration curve of the confocal microscope (Morris *et al.*, 2019). A similar approach was employed to measure the number of myosin and formin molecules.

The number of actin filaments in a cross-section of the contractile ring was calculated by dividing the total length of actin filaments in the ring with the circumference of a cell. The length of actin filaments (µm) equals the number of actin molecules divided by 370. The circumference of wild-type and *adf1-M3* cells was measured at 10 and 13 µm, respectively (Chen and Pollard, 2011). The center-to-center spacing between actin filaments is assumed to be 15 nm (Kanbe *et al.*, 1989; Swulius *et al.*, 2018) in estimating the width of a contractile ring.

Western blots

For probing the expression level of GFP-Lifeact, exponentially growing cells (50 ml) were harvested by centrifugation at 3000 rpm for 5 min. The pellet was resuspended in 300 µl of lysis buffer (50 mM Tris-HCl, 100 mM KCl, 3 mM $MgCl_2$, 1 mM EDTA, 1 mM dithiothreitol, and 0.1% Triton X-100) containing Halt protease inhibitor cocktail (100×; #1862209; Thermo-Fisher Scientific) and frozen at –20°C. The cells were mechanically lysed using a BeadBug microtube homogenizer (Benchmark Scientific). Protein samples were resolved by Mini-PROTEAN TGX Precast SDS–PAGE gels (#4561084; BioRad). The gels were either stained with Coomassie blue or transferred to PVDF (polyvinylidene fluoride) membrane (Millipore) for immunoblots. The blots were first incubated with the anti-GFP antibody (1:1000 diluted; #11814460001; Sigma-Roche) overnight at 4°C, followed by horseradish peroxidase–linked secondary antibody (1:5000; #sc-516102; Santa Cruz) for 2 h at room temperature. Blots were developed with SuperSignal West Pico PLUS chemiluminescent substrate (#34577; Thermo-Fisher Scientific).

ACKNOWLEDGMENTS

Research reported in this publication was supported by the National Institute of General Medical Sciences of the National Institutes of Health under award numbers R01GM026132 to T.D.P. and R15GM134496 to Q.C. The content is solely the responsibility of the authors and does not necessarily represent the official views of the National Institutes of Health. We thank Debatrayee Sinha and Abhishek Poddar for technical assistance.

REFERENCES

Bezanilla M, Wilson JM, Pollard TD (2000). Fission yeast myosin-II isoforms assemble into contractile rings at distinct times during mitosis. Curr Biol 10, 397–400.

Bohnert KA, Grzegorzewska AP, Willet AH, Vander Kooi CW, Kovar DR, Gould KL (2013). SIN-dependent phosphoinhibition of formin multimerization controls fission yeast cytokinesis. Genes Dev 27, 2164–2177.

Cao LG, Wang YL (1990a). Mechanism of the formation of contractile ring in dividing cultured animal cells. I. Recruitment of preexisting actin filaments into the cleavage furrow. J Cell Biol 110, 1089–1095.

Cao LG, Wang YL (1990b). Mechanism of the formation of contractile ring in dividing cultured animal cells. II. Cortical movement of microinjected actin filaments. J Cell Biol 111, 1905–1911.

Chang F, Woollard A, Nurse P (1996). Isolation and characterization of fission yeast mutants defective in the assembly and placement of the contractile actin ring. J Cell Sci 109 (Pt 1), 131–142.

Cheffings TH, Burroughs NJ, Balasubramanian MK (2019). Actin turnover ensures uniform tension distribution during cytokinetic actomyosin ring contraction. Mol Biol Cell 30, 933–941.

Chen Q, Nag S, Pollard TD (2012). Formins filter modified actin subunits during processive elongation. J Struct Biol 177, 32–39.

Chen Q, Pollard TD (2011). Actin filament severing by cofilin is more important for assembly than constriction of the cytokinetic contractile ring. J Cell Biol 195, 485–498.

Chen Q, Pollard TD (2013). Actin filament severing by cofilin dismantles actin patches and produces mother filaments for new patches. Curr Biol 23, 1154–1162.

Coffman VC, Sees JA, Kovar DR, Wu JQ (2013). The formins Cdc12 and For3 cooperate during contractile ring assembly in cytokinesis. J Cell Biol 203, 101–114.

Courtemanche N, Pollard TD, Chen Q (2016). Avoiding artefacts when counting polymerized actin in live cells with LifeAct fused to fluorescent proteins. Nat Cell Biol 18, 676–683.

Ghosh M, Song X, Mouneimne G, Sidani M, Lawrence DS, Condeelis JS (2004). Cofilin promotes actin polymerization and defines the direction of cell motility. Science 304, 743–746.

Goss JW, Kim S, Bledsoe H, Pollard TD (2014). Characterization of the roles of Blt1p in fission yeast cytokinesis. Mol Biol Cell 25, 1946–1957.

Guha M, Zhou M, Wang YL (2005). Cortical actin turnover during cytokinesis requires myosin II. Curr Biol 15, 732–736.

Huang J, Huang Y, Yu H, Subramanian D, Padmanabhan A, Thadani R, Tao Y, Tang X, Wedlich-Soldner R, Balasubramanian MK (2012). Nonmedially assembled F-actin cables incorporate into the actomyosin ring in fission yeast. J Cell Biol 199, 831–847.

Kanbe T, Kobayashi I, Tanaka K (1989). Dynamics of cytoplasmic organelles in the cell cycle of the fission yeast Schizosaccharomyces pombe: three-dimensional reconstruction from serial sections. J Cell Sci 94 (Pt 4), 647–656.

Khaliullin RN, Green RA, Shi LZ, Gomez-Cavazos JS, Berns MW, Desai A, Oegema K (2018). A positive-feedback-based mechanism for constriction rate acceleration during cytokinesis in Caenorhabditis elegans. eLife 7, e36073.

Konzok A, Weber I, Simmeth E, Hacker U, Maniak M, Muller-Taubenberger A (1999). DAip1, a Dictyostelium homologue of the yeast actin-interacting protein 1, is involved in endocytosis, cytokinesis, and motility. J Cell Biol 146, 453–464.

Kovar DR, Kuhn JR, Tichy AL, Pollard TD (2003). The fission yeast cytokinesis formin Cdc12p is a barbed end actin filament capping protein gated by profilin. J Cell Biol 161, 875–887.

Laplante C, Berro J, Karatekin E, Hernandez-Leyva A, Lee R, Pollard TD (2015). Three myosins contribute uniquely to the assembly and constriction of the fission yeast cytokinetic contractile ring. Curr Biol 25, 1955–1965.

Laplante C, Huang F, Tebbs IR, Bewersdorf J, Pollard TD (2016). Molecular organization of cytokinesis nodes and contractile rings by super-resolution fluorescence microscopy of live fission yeast. Proc Natl Acad Sci USA 113, E5876–E5885.

Lukinavicius G, Reymond L, D'Este E, Masharina A, Gottfert F, Ta H, Guther A, Fournier M, Rizzo S, Waldmann H, *et al.* (2014). Fluorogenic

probes for live-cell imaging of the cytoskeleton. Nat Methods 11, 731–733.
Morris Z, Sinha D, Poddar A, Morris B, Chen Q (2019). Fission yeast TRP channel Pkd2p localizes to the cleavage furrow and regulates cell separation during cytokinesis. Mol Biol Cell 30, 1791–1804.
Murthy K, Wadsworth P (2005). Myosin-II-dependent localization and dynamics of F-actin during cytokinesis. Curr Biol 15, 724–731.
Nakano K, Mabuchi I (2006). Actin-capping protein is involved in controlling organization of actin cytoskeleton together with ADF/cofilin, profilin and F-actin crosslinking proteins in fission yeast. Genes Cells 11, 893–905.
Okada H, Wloka C, Wu JQ, Bi E (2019). Distinct roles of myosin-II isoforms in cytokinesis under normal and stressed conditions. iScience 14, 69–87.
Okreglak V, Drubin DG (2007). Cofilin recruitment and function during actin-mediated endocytosis dictated by actin nucleotide state. J Cell Biol 178, 1251–1264.
Pollard TD, O'Shaughnessy B (2019). Molecular mechanism of cytokinesis. Annu Rev Biochem 88, 661–689.
Riedl J, Crevenna AH, Kessenbrock K, Yu JH, Neukirchen D, Bista M, Bradke F, Jenne D, Holak TA, Werb Z, *et al*. (2008). Lifeact: a versatile marker to visualize F-actin. Nat Methods 5, 605–607.
Schroeder TE (1972). The contractile ring. II. Determining its brief existence, volumetric changes, and vital role in cleaving Arbacia eggs. J Cell Biol 53, 419–434.
Stachowiak MR, Laplante C, Chin HF, Guirao B, Karatekin E, Pollard TD, O'Shaughnessy B (2014). Mechanism of cytokinetic contractile ring constriction in fission yeast. Dev Cell 29, 547–561.
Straight AF, Cheung A, Limouze J, Chen I, Westwood NJ, Sellers JR, Mitchison TJ (2003). Dissecting temporal and spatial control of cytokinesis with a myosin II Inhibitor. Science 299, 1743–1747.
Swulius MT, Nguyen LT, Ladinsky MS, Ortega DR, Aich S, Mishra M, Jensen GJ (2018). Structure of the fission yeast actomyosin ring during constriction. Proc Natl Acad Sci USA 115, E1455–E1464.
Takaine M, Numata O, Nakano K (2015). An actin-myosin-II interaction is involved in maintaining the contractile ring in fission yeast. J Cell Sci 128, 2903–2918.
Thevenaz P, Ruttimann UE, Unser M (1998). A pyramid approach to subpixel registration based on intensity. IEEE Trans Image Process 7, 27–41.
Vavylonis D, Wu J-Q, Hao S, O'Shaughnessy B, Pollard TD (2008). Assembly mechanism of the contractile ring for cytokinesis by fission yeast. Science 319, 97–100.
Wang N, Lee IJ, Rask G, Wu JQ (2016). Roles of the TRAPP-II complex and the exocyst in membrane deposition during fission yeast cytokinesis. PLoS Biol 14, e1002437.
White JG, Borisy GG (1983). On the mechanisms of cytokinesis in animal cells. J Theor Biol 101, 289–316.
Wu JQ, Kuhn JR, Kovar DR, Pollard TD (2003). Spatial and temporal pathway for assembly and constriction of the contractile ring in fission yeast cytokinesis. Dev Cell 5, 723–734.
Wu JQ, Pollard TD (2005). Counting cytokinesis proteins globally and locally in fission yeast. Science 310, 310–314.
Zambon P, Palani S, Kamnev A, Balasubramanian MK (2017). Myo2p is the major motor involved in actomyosin ring contraction in fission yeast. Curr Biol 27, R99–R100.
Zhang XF, Hyland C, Van Goor D, Forscher P (2012). Calcineurin-dependent cofilin activation and increased retrograde actin flow drive 5-HT-dependent neurite outgrowth in Aplysia bag cell neurons. Mol Biol Cell 23, 4833–4848.
Zimmermann D, Homa KE, Hocky GM, Pollard LW, De La Cruz EM, Voth GA, Trybus KM, Kovar DR (2017). Mechanoregulated inhibition of formin facilitates contractile actomyosin ring assembly. Nat Commun 8, 703.